EUKARYOTIC CELL, Feb. 2011, p. 276–283 Vol. 10, No. 2
1535-9778/11/$12.00 doi:10.1128/EC.00224-10

The *Aspergillus nidulans nucA*^{EndoG} Homologue Is Not Involved in Cell Death$^{\nabla}$

Bárbara de Castro Pimentel Figueiredo,[1] Patrícia Alves de Castro,[1] Taísa Magnani Dinamarco,[1] Maria Helena S. Goldman,[2] and Gustavo Henrique Goldman[1,3]*

Faculdade de Ciências Farmacêuticas de Ribeirão Preto[1] and Faculdade de Filosofia, Ciências e Letras de Ribeirão Preto,[2] Universidade de São Paulo, São Paulo, Brazil, and Laboratório Nacional de Ciência e Tecnologia do Bioetanol, CTBE, Caixa Postal 6170, 13083-970 Campinas, São Paulo, Brazil[3]

Received 14 September 2010/Accepted 8 November 2010

Upon apoptosis induction, translocation of mammalian mitochondrial endonuclease G (EndoG) to the nucleus coincides with large-scale DNA fragmentation. Here, we describe for the first time a homologue of EndoG in filamentous fungi by investigating if the *Aspergillus nidulans* homologue of the EndoG gene, named *nucA*^{EndoG}, is being activated during farnesol-induced cell death. Our results suggest that NucA is not involved in cell death, but it plays a role in the DNA-damaging response in *A. nidulans*.

The mechanisms involved in cell death in filamentous fungi are not well known (for reviews, see references 9, 17, and 24). We have been using *Aspergillus nidulans* and the isoprenoid farnesol (FOH), which inhibits proliferation and induces apoptosis, as a model system and cell death stimulus, respectively, aiming to understand by which means filamentous fungi are driven toward cell death (3, 5, 20, 23). In mammalian cells, at least two major apoptotic pathways have been depicted: (i) the intrinsic pathway, which needs the involvement of the mitochondria, and (ii) the extrinsic pathway, where mitochondria are bypassed and caspases are activated (for a review, see reference 6). One of the hallmarks of the intrinsic pathway is the release of apoptogenic factors, such as cytochrome *c*, to the cytosol and the consequent assembly, organized by this protein, of the high-molecular-weight complex, the mitochondrial apoptosome, which activates caspases (for a review, see reference 6). In *Saccharomyces cerevisiae* cells undergoing an apoptotic process induced by acetic acid, translocation of Cyc1p to the cytosol was observed (13). Another factor of the intrinsic pathway is endonuclease G (EndoG), which has been described as a mitochondrial endonuclease that digests both DNA and RNA (1, 2). Upon apoptosis induction, translocation of mammalian EndoG and its *S. cerevisiae* homologue *NUC1* to the nucleus coincides with large-scale DNA fragmentation (2, 12, 16). Here, we describe for the first time a homologue of EndoG in filamentous fungi by investigating if the *A. nidulans* EndoG homologue, named *nucA*^{EndoG}, is being activated during FOH-induced cell death.

We identified AN2185.2 as the putative homologue of *S. cerevisiae NUC1* (53% identity, 68% similarity, E value of 2e−97). *In silico* analysis of NucA (Fig. 1A) shows a putative mitochondrial target sequence (MTS) located at amino acids 1 to 28 (as predicted by MITOPROT [http://ihg.gsf.de/ihg/mitoprot.html], PrediSi [http://www.predisi.de/home.html], and Predotar [http://urgi.versailles.inra.fr/predotar/predotar.html]) and a putative nuclear localization signal located at amino acids 308 to 314 (as predicted by NucPred [http://www.sbc.su.se/~maccallr/nucpred/] but not confirmed by NetNES 1.1 [http://www.cbs.dtu.dk/services/NetNES-1.1/index.php] or by PredictNLS Server [http://cubic.bioc.columbia.edu/services/predictNLS/]). A DNA/RNA nonspecific endonuclease active site (PS01070; http://www.expasy.org/prosite/), typical of a family of bacterial and eukaryotic endonucleases that cleave double-stranded and single-stranded nucleic acids and require a divalent ion such as magnesium for their activity, is located at amino acids 156 to 164 (Fig. 1A).

For total RNA isolation, RNase-free DNase I treatment for the real-time PCR experiments and the reactions and calculations were performed according to the method described in reference 22. Primers and Lux probes for the normalizer β-tubulin (*tubC*) are 5′-GCAGAATGTCTCGTCCGAATG-3′ and 5′-CACTTTATGCCGTCGCCGAAAG[FAM]G-3 (where FAM is 6-carboxyfluorescein), while for *nucA*^{EndoG} the primers and Lux probes are 5′-cggatTGGTGGCCTCTGTCATATCc[FAM]G-3′ and 5′-GCCTCTCTTCCGTGCCAAACT-3′. When the wild-type strain is exposed to FOH, there is an increased accumulation of *nucA*^{EndoG} mRNA of 3.1-, 40.0-, and 10.8-fold at 10, 50, and 100 μM FOH, respectively (Fig. 1B). There is a low *nucA*^{EndoG} mRNA accumulation when *A. nidulans* germlings were exposed to oxidative stressing agents, such as hydrogen peroxide and paraquat (about 2.0- and 3.5-fold at 100 mM H_2O_2 and 5 mM paraquat, both for 60 min, respectively) (Fig. 1C), and DNA-damaging agents (about 2- to 3-fold for hydroxyurea [HU], methyl methanesulfonate [MMS], and bleomycin [BLEO]) (Fig. 1D).

Standard genetic techniques for *A. nidulans* were used for all strain constructions and transformations (11). DNA manipulations were as described in reference 19. All PCRs were performed using Platinum *Taq* DNA Polymerase High Fidelity (Invitrogen). For the DNA-mediated transformation, the deletion and monomeric red fluorescent protein (mRFP) fusion cassettes were constructed by *in vivo* recombination in *S. cerevisiae* as previously described in reference

* Corresponding author. Mailing address: Departamento de Ciências Farmacêuticas, Faculdade de Ciências Farmacêuticas de Ribeirão Preto, Universidade de São Paulo, Av. do Café S/N, CEP 14040-903, Ribeirão Preto, São Paulo, Brazil. Phone and fax: 55-16-36024280/81. E-mail: ggoldman@usp.br.

$^{\nabla}$ Published ahead of print on 3 December 2010.

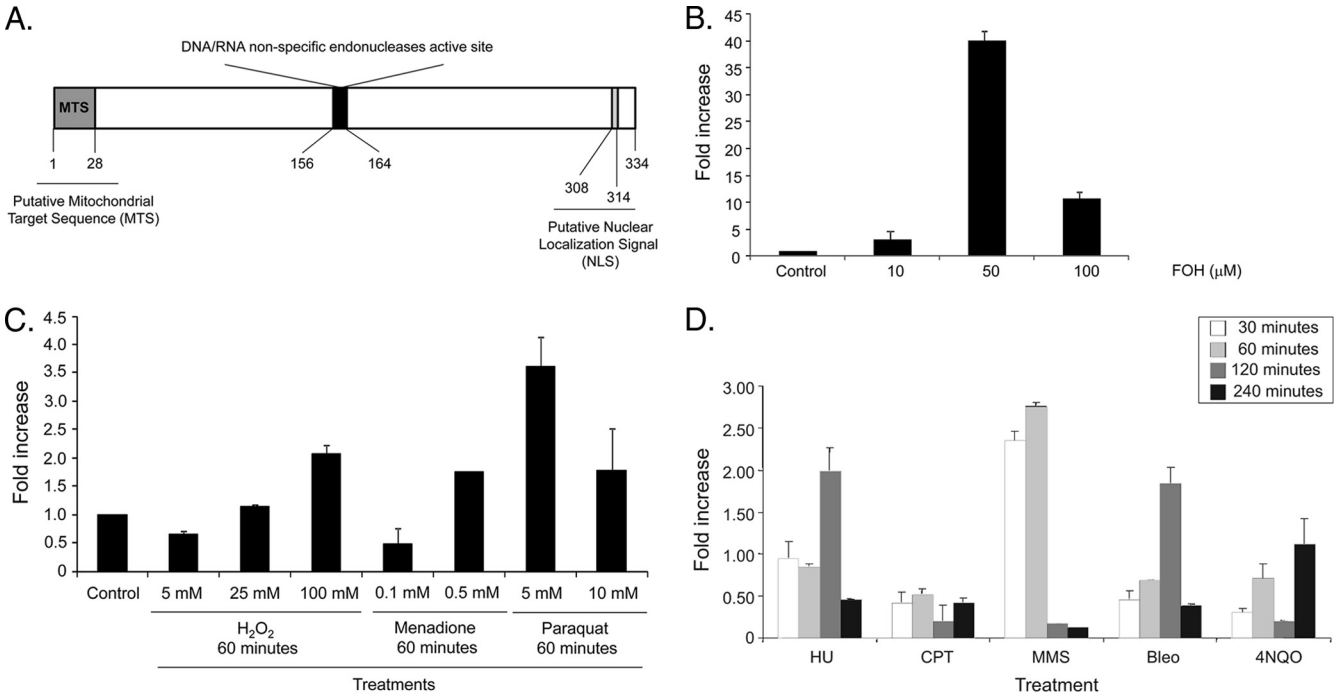

FIG. 1. *In silico* analysis of NucA (A) and expression levels of the *nucA*^{EndoG} gene (B to D). The wild-type strain was grown for 16 h in YG at 37°C and transferred to fresh YG with FOH (0, 10, 50, or 100 μM FOH for 2 h) (B), oxidative stressing agents (C), or DNA-damaging agents (25 μM camptothecin [CPT], 0.003% methyl methanesulfonate [MMS], 0.6 μg/ml bleomycin [BLEO], or 0.25 μg/ml 4-nitroquinoline oxide [4-NQO] for 30, 60, 120, and 240 min) (D). The relative quantitation of *nucA*^{EndoG} and tubulin gene expression was determined by a standard curve (i.e., threshold cycle [C_T] values plotted against logarithm of the DNA copy number). The results are the means ± standard deviations from four sets of experiments. The values represent the fold change in gene expression compared to that of the wild-type control grown without any drug (represented absolutely as 1.00).

4. Briefly, for the gene deletion, about 1.5-kb regions on either side of the open reading frames (ORFs) were selected for primer design (5′-gtaacgccagggttttcccagtcacgacgGTTGATG ATATGGAACTCGTGCTTGTCG-3′, 5′-GACCCAACAA CCATGATACCATCGTTGCTGTGGATTGAAAAAATG GAGAA-3′, 5′-CTGTCGATCATGTGGATGCTACGGCT ACTGTACATCTATATCATACCTATCTGT-3′, and 5′-gcgg ataacaatttcacacaggaaacagcCTAGGCCAGTGTCCGAACTA CAAACC-3′ [lowercase letters indicate homology with the pRS426 vector region]). The NucA::mRFP cassette was constructed by using the primers 5′-gtaacgccagggttttcccagtcacgacg GTCATCGACCCCAGCATCCC-3′, 5′-GCTCCAGCGCCT GCACCAGCTCCAGCCTTCTTCTTCGCATTGTTAAACT CC-3′, 5′-GACCCAACAACCATGATACCATTGCTGTTG CCAGGTGAGG-3′, and 5′-GGACTGGTGCAGGCGCTG GAGC-3′. The CycA::mRFP cassette was constructed by using the primers 5′-acgccagggttttcccagtcacgacgTTGTTATTACGG GGAGGGCTACTCCGG-3′, 5′-GCTCCAGCGCCTGCACC AGCTCCAGAGGCCCGGCGATCCC-3′, 5′-CTGTCGATC ATGTGGATGCTGTGACAGGCGGGTACTGTAACATT ACACC-3′, and 5′-gcggataacaatttcacacaggaaacAGCAGCGG TGGCGATTACTTGTGTTC-3′. Fragments of 5′ and 3′ untranslated regions of each gene were PCR amplified from genomic DNA using the A4 strain as the template for *A. nidulans* cassettes. The *pyroA* gene used in the *A. nidulans* cassette for generating the Δ*nucA*, *alcA*::*nucA*, NucA::mRFP, and CycA::mRFP strains was amplified from *A. fumigatus* Af293. Cassette generation was achieved by transforming each fragment for each construction along with the plasmid pRS426 BamHI/EcoRI cut in the in *S. cerevisiae* strain SC9721 by the lithium acetate method (21). The DNA of the yeast transformants was extracted by the method described in reference 8, dialyzed, and transformed by electroporation in *Escherichia coli* strain DH10B to rescue the pRS426 plasmid harboring the cassettes. The cassettes were PCR amplified from these plasmids and used for transformation of *Aspergilli* according to the procedure described in reference 15. Transformants were scored for their ability to grow on minimal medium. PCR or Southern blot analyses were used throughout this study to demonstrate that the transformation cassettes had integrated homologously at the targeted *A. nidulans* loci.

We constructed a deletion mutant for *nucA*^{EndoG} (Fig. 2A). We investigated the effects of overexpressing *nucA*^{EndoG} in *A. nidulans* by constructing a conditional *alcA* mutant of the *nucA*^{EndoG} gene (Fig. 2B), using the primers 5′ CCCGGTAC CGCTAATTAACT 3′, 5′ CTGTCGATCATGTGGATGCTA AAAGCTGATTGTGATAGTTCCC 3′, 5′ AGTTAATTAG CGGTACCGGGATGTCCAAGGCCACTGTTGCTG 3′, and 5′ GCGGATAACAATTTCACACAGGAAACAGCCTAGGC CAGTGTCCGAACTACAAACC 3′. The *alcA* promoter is repressed by glucose, derepressed by glycerol, and induced to high levels by ethanol or L-threonine (7). The *nucA*^{EndoG} deletion strain has no apparent growth or conidiation defects and did not show increased susceptibility to FOH (Fig. 2C, left). Overexpres-

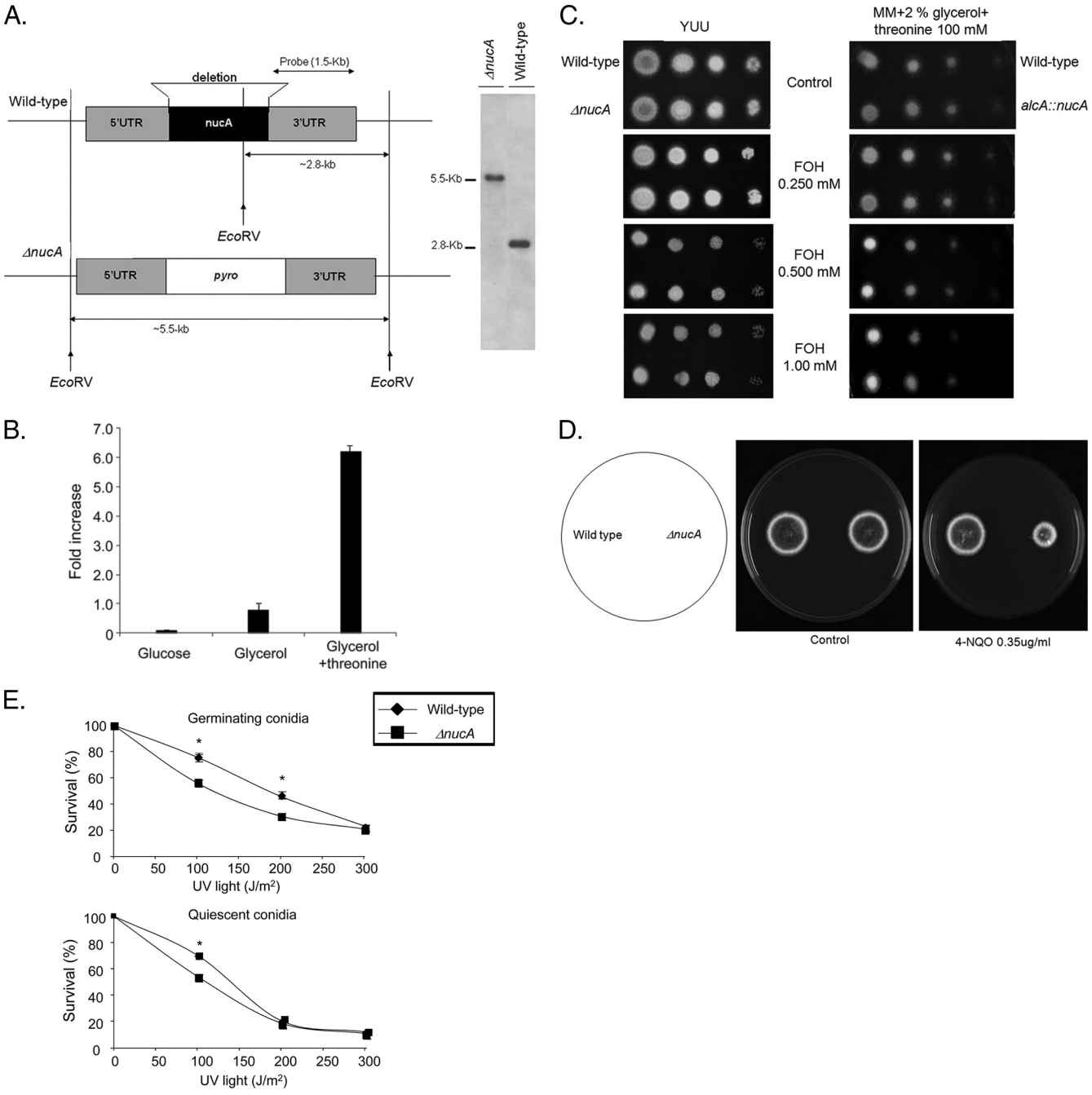

FIG. 2. Phenotypes of the Δ*nucA* deletion strain. (A) Schematic illustration of the *nucA*$^{\mathrm{EndoG}}$ deletion strategy. Genomic DNA from both wild-type and Δ*nucA* strains was isolated and cleaved with the enzyme EcoRV; a 1.5-kb DNA fragment was used as a hybridization probe. This fragment recognizes a single DNA band (about 2.8 kb) in the wild-type strain and also a single DNA band (about 5.5 kb) in the Δ*nucA* mutant, as shown in the Southern blot analysis. (B) Expression of *nucA*$^{\mathrm{EndoG}}$ in the *alcA*::*nucA* strain. The *alcA*::*nucA* strain was grown for 16 h at 37°C in 2% minimal medium (MM) plus glycerol. After this period, mycelia were transferred to MM plus different carbon sources and grown for another 6 h at 37°C. The relative *nucA*$^{\mathrm{EndoG}}$ quantitation was performed as described for Fig. 1. (C) FOH susceptibility of Δ*nucA* and *alcA*::*nucA* mutants. Aliquots (5 μl) of 10-fold dilutions derived from a starting suspension of 1.0×10^8 conidia/ml of the corresponding wild-type, Δ*nucA*, and *alcA*::*nucA* strains were spotted on YG agar plates supplemented with 0, 0.25, 0.5, or 1.0 mM FOH. The plates were incubated at 37°C for 48 h. (D) Growth phenotypes of the wild-type and *nucA*$^{\mathrm{EndoG}}$ deletion mutant strains grown either in complete medium (YG) supplemented with uridine and uracyl (YUU) or in YUU plus 0.35 μg/ml of 4-NQO for 48 h at 37°C. (E) Quiescent and germinating conidiospores from different strains were exposed to UV light, and viability was scored after exposure to this DNA-damaging agent. Viability was determined as the percentage of colonies on treated plates compared to that on untreated controls. The results are the means ± standard deviations from four independent experiments. Statistical differences were determined by one-way analysis of variance (ANOVA) followed, when significant, by the Newman-Keuls multiple comparison test, using Sigma Stat statistical software (Jandel Scientific). *, $P < 0.01$.

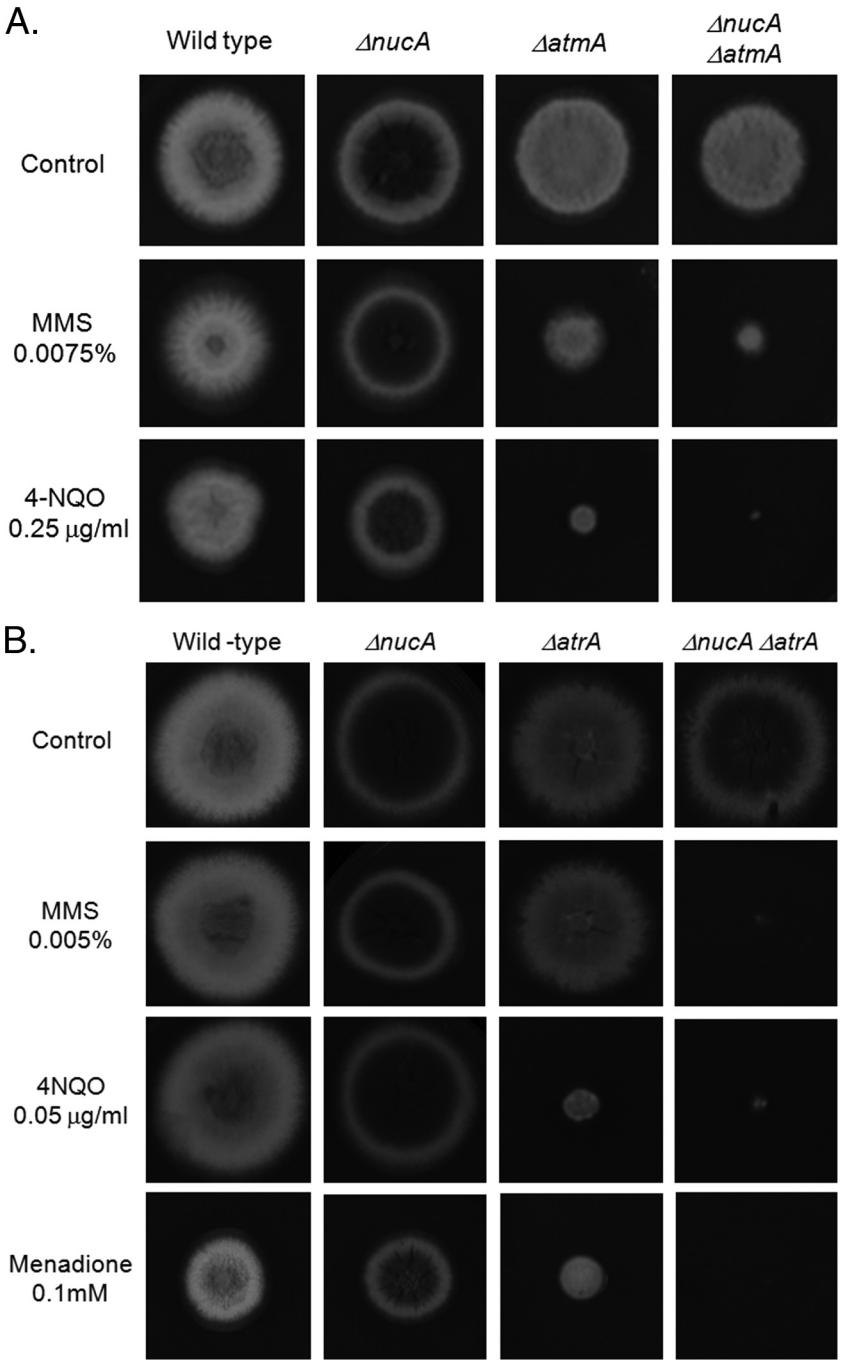

FIG. 3. Genetic interactions with the *A. nidulans* Δ*nucA* mutant. (A) Growth phenotypes of the wild-type, Δ*nucA*, Δ*atrA*, and Δ*nucA* Δ*atrA* strains grown in YUU, YUU plus MMS (0.0075%), or YUU plus 4-NQO (0.25 μg/ml). (B) Growth phenotypes of the wild-type, Δ*nucA*, Δ*atmA*, and Δ*nucA* Δ*atmA* strains grown in YUU, YUU plus MMS (0.005%), YUU plus 4-NQO (0.25 μg/ml), or YUU plus menadione (0.1 mM).

sion of the *nucA*$^{\mathrm{EndoG}}$ gene (about 7-fold at 10 μM FOH; see Fig. 2B) did not increase the susceptibility to FOH (Fig. 2C, right). To verify if the *nucA*$^{\mathrm{EndoG}}$ deletion and overexpression mutants are more sensitive to cell death caused by other stressing agents, we exposed conidia of these strains to several concentrations/dosages of amphotericin, itraconazole, caspofungin, camptothecin, hydroxyurea, sirolimus, calcium, menadione, hydrogen peroxide, and paraquat. We were not able to observe any other phenotype of susceptibility to these agents. However, the *nucA*$^{\mathrm{EndoG}}$ deletion mutant is more sensitive to 4-nitroquinoline oxide (Fig. 2D), and its quiescent and germinating conidia are slightly more sensitive to UV light (Fig. 2E).

ATM and ATR are paralogous phosphoinositide 3-kinase-related kinases (PIKKs) that orchestrate the DNA damage response in eukaryotic cells (14, 25). Aiming to see possible interactions between NucA and other elements of the DNA

damage response, we constructed Δ*nucA* double mutants with Δ*atmA*^{ATM} and Δ*uvsB*^{ATR}, the *A. nidulans* ATM and ATR gene homologues. We have tested comparatively their growth in the presence of several DNA-damaging agents. The Δ*nucA* Δ*atmA*^{ATM} double mutant was more sensitive to 0.0075% methyl methanesulfonate and 0.25 μg/ml 4-nitroquinoline oxide (Fig. 3A). The Δ*nucA* and Δ*uvsB*^{ATR} double mutants were more sensitive to 0.005% MMS, 0.05 μg/ml 4-NQO, and 0.1 mM menadione (Fig. 3B). These results indicate that NucA is genetically interacting with these two genes, aiming to repair DNA damage caused by these genotoxins. Taken together, all these results suggest that NucA does not seem to be involved in cell death, but it plays a role in the DNA-damaging response in *A. nidulans*.

We also constructed a NucA::mRFP strain that has the same degree of FOH sensitivity as the wild strain (data not shown) and exposed it to FOH. NucA::mRFP accumulation was detected along the cytoplasm but not in the nuclei when NucA::mRFP germlings were exposed or not to FOH (Fig. 4A). The same results were observed when NucA::mRFP was exposed to different concentrations of 4-NQO (data not shown). Since our microscopic localization studies did not allow us to assess the subcellular location of NucA::mRFP, we decided to perform cell fractionation studies. For the extraction of mitochondrial proteins, mitochondria were isolated from *A. nidulans* mycelium based on the method described in reference 26. Germlings grown for 16 h (at 30°C) exposed or not to 500 μM FOH for 2 h at 30°C were ground with liquid nitrogen and resuspended in 50 ml ice-cold isolation buffer (0.4 M mannitol, 0.1% [wt/vol] bovine serum albumin [BSA], 1 mM EGTA, 15 mM β-mercaptoethanol, and 0.05 mM phenylmethylsulfonyl fluoride [PMSF] in 25 mM morpholinepropanesulfonic acid [MOPS] buffer, pH 7.8). Mitochondria were enriched as follows. Cell debris was spun down three times at 3,000 × *g* for 5 min, and then a centrifugation step at 18,000 × *g* for 30 min followed. The mitochondrial fraction was carefully resuspended in 3 ml of resuspension buffer (0.4 M mannitol, 1 mM EGTA, 0.2 mM PMSF, and 10 mM KH_2PO_4-KOH, pH 7.2) and homogenized with two strokes in an Elvehjem-Potter homogenizer. This resuspension was layered on top of a three-step Percoll gradient (10 ml of 14% [vol/vol], 10 ml of 26% [vol/vol], and 5 ml of 45% [vol/vol] Percoll in 0.4 M mannitol, 1 mM EGTA, and 10 mM KH_2PO_4-KOH, pH 7.2). After centrifugation for 60 min at 47,000 × *g*, mitochondria were isolated from the 26%/45% interphase. To remove Percoll, purified mitochondria were centrifuged twice in resuspension buffer for 30 min at 18,000 × *g*. Both the cytoplasm and the purified organelles were finally resuspended in resuspension buffer.

Each sample assayed for the fluorescence intensity for monomeric red fluorescent protein (mRFP) (excitation, 543 nm; emission, scan from 400 to 700 nm, peaking at 550 nm) was detected by using an F4500 Hitachi fluorescence spectrophotometer. First, we used an *A. nidulans* protein located in the mitochondria, CycA::mRFP (*cycA* gene, AN6246.3, encodes cytochrome *c*), as a positive control for our cell fractionation studies. As expected, CycA::mRFP is located mainly in the mitochondria when CycA::mRFP germlings were exposed or not to FOH, although it showed about twice as much fluorescence when exposed to FOH (Fig. 4B). Interestingly, there is an increase of the *cycA* mRNA accumulation when wild-type germlings were exposed to FOH (about 3.5, 13.3, and 7.0 times more mRNA accumulation when germlings were exposed to 10, 50, and 100 μM FOH, respectively). Cell fractionation studies showed that NucA::mRFP localizes to the mitochondria when NucA::mRFP germlings were exposed or not to FOH (Fig. 4B). Accordingly, there is an induction of about 2.5-fold in the mRFP fluorescence in the mitochondria when NucA::mRFP germlings were exposed to FOH (Fig. 4B). A cytoplasmic marker (mRFP::KipB) was used as a positive control for a protein specifically located in the cytoplasm (Fig. 4B). The *kipB* gene is not induced by FOH and encodes an *A. nidulans* kinesin that localizes to cytoplasmic astral and mitotic microtubules in a discontinuous pattern, and spots of red fluorescent protein move along microtubules toward the plus ends (18). As expected, mRFP::KipB is located predominantly in the cytoplasm (Fig. 4B). Interestingly, our cell fractionation studies suggested that CycA::mRFP does not translocate from the mitochondria to the cytoplasm when germlings were exposed to FOH. The NucA mitochondrial localization was validated by colocalization studies of NucA::mRFP with the mitochondria by using the mitochondrion-specific dye MitoTracker green (Fig. 4C). In the absence of FOH, NucA::mRFP colocalizes to mitochondrial filament-like structures, while when germlings were exposed to 100 μM FOH for either 30 or 120 min, the NucA::mRFP colocalizes to mitochondrial fragment-like structures. Taken together, these results strongly suggest that NucA localizes to the mitochondria exposed or not to FOH.

Aiming to confirm the subcellular localization of cytochrome *c*, another set of cell fractionation studies was performed with the wild-type strain, and the samples were then analyzed by 15% sodium dodecyl sulfate-polyacrylamide gel electrophoresis (SDS-PAGE). Samples were prepared for SDS-PAGE by the addition of 1× sample buffer (62.5 mM Tris-HCl [pH 6.8], 2% SDS, 10% glycerol, 5% β-mercaptoethanol, and 5% bromophenol blue) and heating at 100°C for 3 min. Twenty micrograms of total protein from each sample was loaded into each lane of a 15% SDS-PAGE gel. After separation of the proteins, the gel was blotted onto a pure nitrocellulose membrane (0.2 μm; Bio-Rad), and after being blocked in 5% dried milk in TBS-T buffer (10 mM Tris-HCl, 150 mM NaCl [pH 8.0], and 0.05% Tween 20), the membrane was probed with the rabbit anti-cyc1 antibody (CNAT; against native cytochrome *c* from yeast; Sigma) at a 1:200 dilution in TBS-T buffer for 1 h at room temperature. The membrane was washed four times for 5 min each with TBS-T buffer and then incubated with a 1:5,000 dilution of goat anti-rabbit IgG peroxidase-labeled (KPL) antibody for 1 h. After being washed, the blot was developed by use of the SuperSignal Ultra chemiluminescence detection system (Pierce) and recorded by the use of Hyperfilm ECL (Amersham Biosciences). The Western blot analysis showed that *A. nidulans* CycA is not translocated to the cytoplasm upon exposure to FOH (Fig. 4D). The images generated were subjected to densitometric analysis of pixel intensity using ImageJ software (http://rsbweb.nih.gov/ij/index.html). By normalizing the protein loading, we were able to see that there is about 2.3 times more protein upon FOH exposure (Fig. 4D). *A. nidulans* NucA localizes predominantly to the mitochondria, but in contrast to its human and yeast homologues, it does not

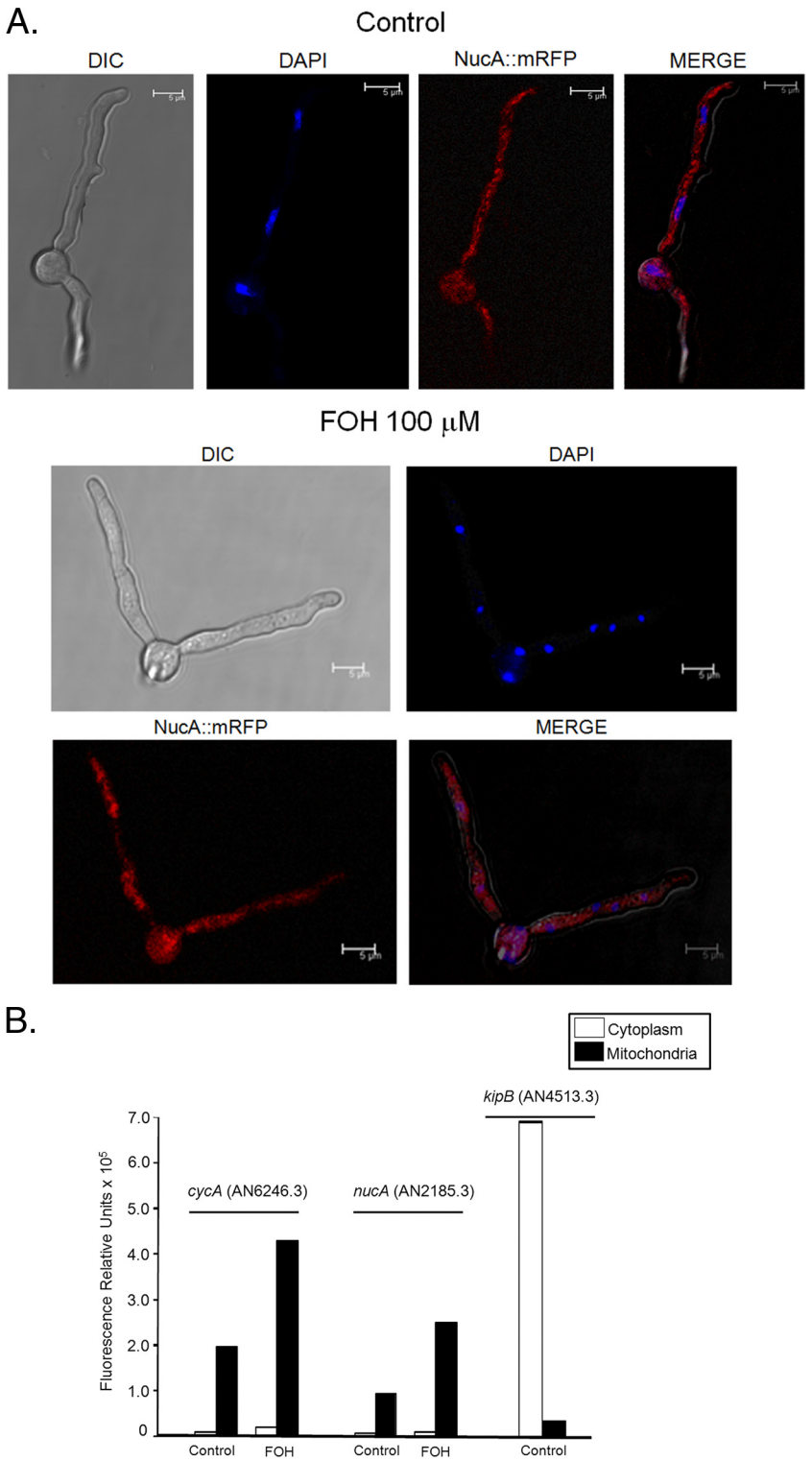

FIG. 4. NucA::mRFP does not translocate to the nucleus upon exposure of germlings to FOH. (A) Germlings of NucA::mRFP were grown in liquid MM for 18 h at 30°C. The 18-h germlings were either not exposed (top, control) or exposed (bottom) to 100 μM FOH for 1 h at 30°C. After the treatment, the germlings were fixed, washed, and DAPI (4′,6-diamidino-2-phenylindole) stained. Samples were analyzed by laser scanning confocal microscopy. Images were captured by direct acquisition. Bars, 5 μm. (B) Cell fractionation studies of the CycA::mRFP and NucA::mRFP strains exposed or not to 500 μM FOH. Graphs are representative of results from at least three independent assays. (C) NucA::mRFP localizes to the mitochondria. This experiment was performed as described in the legend to Fig. 4A. Mitochondrial staining of live cells was performed using MitoTracker green (Invitrogen Molecular Probes). (D) Protein extracts from the wild-type strain (cell fractionation protein assays) were analyzed by Western blotting using antibodies directed against *S. cerevisiae* Cyc1p. Coomassie staining of these protein fractions was used as a loading control by using ImageJ software (http://rsbweb.nih.gov/ij/index.html).

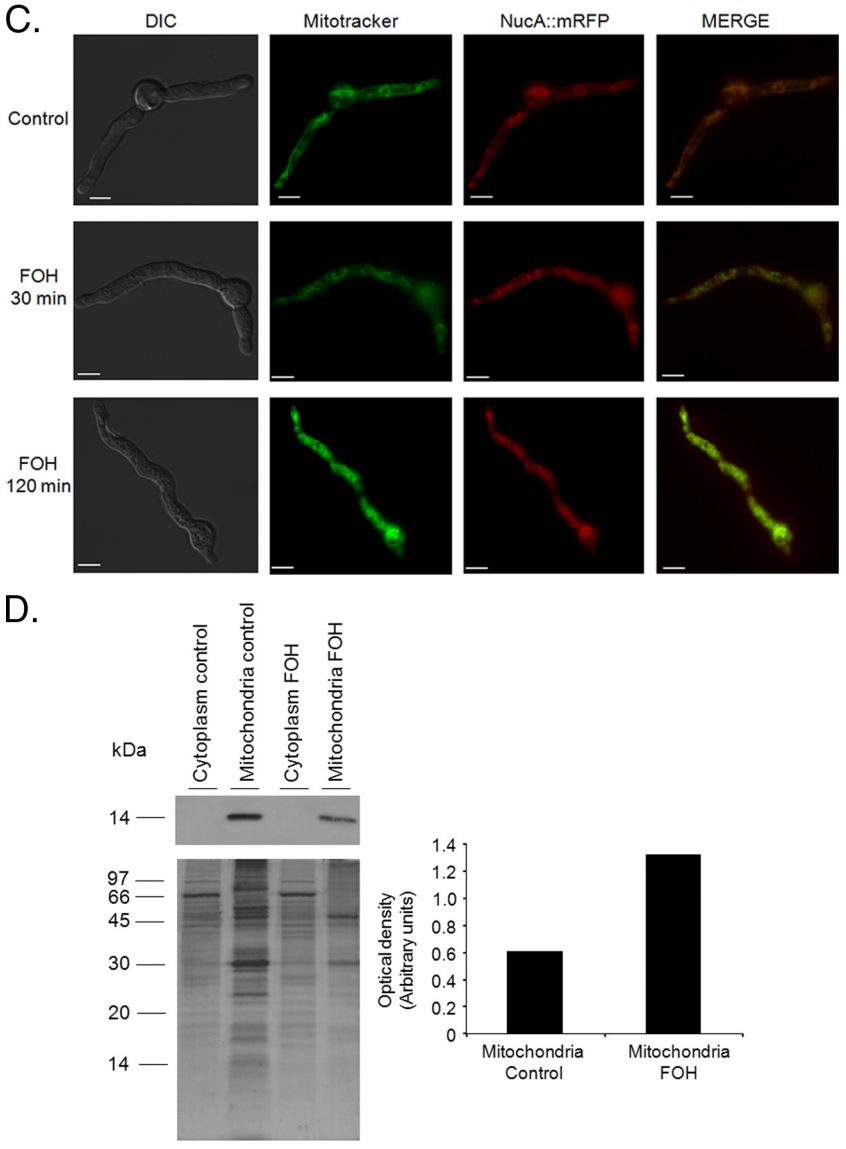

FIG. 4—*Continued.*

migrate to the nucleus upon FOH-induced cell death. The *A. nidulans nucA*$^{\text{EndoG}}$ deletion mutant is sensitive neither to FOH nor to several other cell death inducers. Actually, we investigated a possible role for NucA in DNA damage by constructing double mutants with the two major kinases that participate in signaling during DNA damage, ATM and ATR. There is a synergistic interaction between *A. nidulans* Δ*atmA*, Δ*atrA*, and Δ*nucA* deletion mutants, suggesting that these genes collaborate in parallel pathways for DNA repair. Thus, it is possible that NucA plays a role in mitochondrial recombination and proliferation, as it was previously observed for mammalian cells (10).

During the fractionation studies, we used CycA::mRFP (*cycA* encodes cytochrome *c*) as a positive control for mitochondrial localization. Our results showed that CycA::mRFP is located predominantly in the mitochondria, even when CycA::mRFP germlings were exposed to FOH. Interestingly, during *A. nidulans* FOH-induced cell death, not only is the cytochrome *c* not released to the cytoplasm, but caspases are activated (3). This could reflect a particular feature of the FOH-induced cell death or a more general observation related to cell death in filamentous fungi linked to the fact that regulation and expression of these genes involved in apoptosis could have undergone a rewiring process in mammals during their evolution. However, in *S. cerevisiae* cells undergoing an apoptotic process induced by acetic acid, translocation of CytC to the cytosol and reactive oxygen species (ROS) production were observed (13). The behavior of *A. nidulans* CycA in response to different cell death stimuli remains to be investigated.

In summary, our study shows that the behaviors of two genetic determinants of the intrinsic pathway of cell death in higher eukaryotes, EndoG and cytochrome *c*, are different in FOH-induced cell death in the filamentous fungus *A. nidulans*.

This opens the interesting possibility that cell death in filamentous fungi is activated by distinct (and probably novel) pathways from animals, opening exciting new avenues for research into new targets for the control of fungal proliferation.

This research was supported by the Fundação de Amparo à Pesquisa do Estado de São Paulo (FAPESP), Conselho Nacional de Desenvolvimento Científico e Tecnológico (CNPq), Brazil.

We thank the two anonymous reviewers for their suggestions.

REFERENCES

1. **Burhans, W., and M. Weinberger.** 2007. Yeast endonuclease G: complex matters of death, and of life. Mol. Cell **25:**323–325.
2. **Büttner, S., et al.** 2007. Endonuclease G regulates budding yeast life and death. Mol. Cell **25:**233–246.
3. **Colabardini, A. C., et al.** 2010. Involvement of the *Aspergillus nidulans* protein kinase C with farnesol tolerance is related to the unfolded protein response. Mol. Microbiol. **78:**1259–1279.
4. **Colot, H. V., et al.** 2006. A high-throughput gene knockout procedure for Neurospora reveals functions for multiple transcription factors. Proc. Natl. Acad. Sci. U. S. A. **103:**10352–10357.
5. **Dinamarco, T. M., et al.** 2010. The roles played by Aspergillus nidulans apoptosis-inducing factor (AIF)-like mitochondrial oxidoreductase (AifA) and NADH-ubiquinone oxidoreductases (NdeA-B and NdiA) in farnesol resistance. Fungal Genet. Biol. **47:**1055–1069.
6. **Elmore, S.** 2007. Apoptosis: a review of programmed cell death. Toxicol. Pathol. **35:**45–516.
7. **Flipphi, M., J. Kocialkowska, and B. Felenbok.** 2002. Characteristics of physiological inducers of the ethanol utilization (alc) pathway in *Aspergillus nidulans*. Biochem. J. **15:**25–31.
8. **Goldman, G. H., et al.** 2003. Expressed sequence tag analysis of the human pathogen *Paracoccidioides brasiliensis* yeast phase: identification of putative homologues of *Candida albicans* virulence and pathogenicity genes. Eukaryot. Cell **2:**34–48.
9. **Hamann, A., D. Brust, and H. D. Osiewacz.** 2008. Apoptosis pathways in fungal growth, development and ageing. Trends Microbiol. **16:**276–283.
10. **Huang, K.-J., C.-C. Ku, and I. R. Lehman.** 2006. Endonuclease G: a role for the enzyme in recombination and cellular proliferation. Proc. Natl. Acad. Sci. U. S. A. **103:**8995–9000.
11. **Kafer, E.** 1977. Meiotic and mitotic recombination in *Aspergillus* and its chromosomal aberrations. Adv. Genet. **19:**33–131.
12. **Li, L. Y., X. Luo, and X. Wang.** 2001. Endonuclease G is an apoptotic DNAse when released from mitochondria. Nature **412:**95–99.
13. **Ludovico, P., et al.** 2002. Cytochrome *c* release and mitochondria involvement in programmed cell death induced by acetic acid in *Saccharomyces cerevisiae*. Mol. Biol. Cell **13:**2598–2606.
14. **McKinnon, P. J.** 2004. ATM and ataxia telangiectasia. EMBO Rep. **5:**772–776.
15. **Osmani, S. A., G. S. May, and N. R. Morris.** 1987. Regulation of the mRNA levels of *nimA*, a gene required for the G2-M transition in *Aspergillus nidulans*. J. Cell Biol. **104:**1495–1504.
16. **Parrish, J., et al.** 2001. Mitochondrial endonuclease G is important for apoptosis in *C. elegans*. Nature **412:**90–94.
17. **Ramsdale, M.** 2008. Programmed cell death in pathogenic fungi. Biochim. Biophys. Acta **1783:**1369–1380.
18. **Rischitor, P., S. Konzack, and R. Fischer.** 2004. The Kip3-like kinesin KIPB moves along microtubules and determines spindle position during synchronized mitoses in hyphae of *Aspergillus nidulans*. Eukaryot. Cell **3:**632–645.
19. **Sambrook, J., and D. W. Russell.** 2001. Molecular cloning: a laboratory manual, 3rd ed. Cold Spring Harbor Laboratory Press, Cold Spring Harbor, NY.
20. **Savoldi, M., et al.** 2008. Farnesol induces the transcriptional accumulation of the *Aspergillus nidulans* apoptosis-inducing factor (AIF)-like mitochondrial oxidoreductase. Mol. Microbiol. **70:**44–59.
21. **Schiestl, R. H., and R. D. Gietz.** 1989. High efficiency transformation of intact yeast cells using single stranded nucleic acids as a carrier. Curr. Genet. **16:**339–346.
22. **Semighini, C. P., M. Marins, M. H. S. Goldman, and G. H. Goldman.** 2002. Quantitative analysis of the relative transcript levels of ABC transporter *Atr* genes in *Aspergillus nidulans* by real-time reverse transcription-PCR assay. Appl. Environ. Microbiol. **68:**1351–1357.
23. **Semighini, C. P., M. Savoldi, G. H. Goldman, and S. D. Harris.** 2006. Functional characterization of the putative *Aspergillus nidulans* poly(ADP-ribose) polymerase homolog PrpA. Genetics **173:**87–98.
24. **Sharon, A., A. Finkelstein, N. Shlezingers, and I. Hatam.** 2009. Fungal apoptosis: function, genes and gene function. FEMS Microbiol. Rev. **33:**833–854.
25. **Shiloh, Y., and M. B. Kastan.** 2001. ATM: genome stability, neuronal development, and cancer cross paths. Adv. Cancer Res. **83:**209–254.
26. **Vödisch, M., et al.** 2009. Two-dimensional proteome reference maps for the human pathogenic filamentous fungus *Aspergillus fumigatus*. Proteomics **9:**1407–1415.